Characterization of Organic p/n Junction Photodiodes Based on Poly(alkylthiophene)/Perylene Diimide Bilayers

Li Tan,[†] M. David Curtis,*[,†,‡] and A. H. Francis[‡]

Macromolecular Science & Engineering Center and Department of Chemistry, The University of Michigan, Ann Arbor, Michigan 48109-1055

Received March 20, 2003. Revised Manuscript Received April 4, 2003

Photoconduction of bilayer organic p/n junction photocells can be finely tuned through the alteration of either the side chain orientation (regiorandom vs regioregular) or main chain structure in poly(3-alkylthiophene)s (P3ATs), where the incorporation of an electron-donating group (EDOT) appears to be an excellent method for enhancing the photoconduction. Moreover, doping of P3ATs proved to be an equally viable route for tuning the device characteristics. These polymers were used to fabricate bilayer organic photocells with the polymer as the p-type layer and 1,2-diaminobenzene perylene-3,4,9,10-tetracarboxylic acid diimide (PV) as the n-type layer. Action spectra at steady-state illumination demonstrated that all the interfaces (organic−organic p/n junction and organic−electrode) are actively involved in the photogeneration of carriers. Experiments showed that critical device properties, for example, open-circuit voltage (V_{oc}) and short-circuit current (I_{sc}), are not only dependent on the selection of electrodes and organic materials but also greatly affected by the illumination wavelength and intensity.

Introduction

There is currently a great deal of interest in exploring the application of organic materials, such as conjugated polymers and small molecules, in electronic devices, for example, sensors,[1] electroluminescent devices (LEDs),[2] thin film transistors (TFTs),[3] and photodiodes.[4] Organic materials as the active components possess several advantages over their silicon counterparts, for example, ease of preparation, low processing cost, and a nearly unlimited variability.

Fabrication of organic materials into solar cells or photodiodes is one of the most active areas among these investigations as appreciable photovoltaic effects, for example, open-circuit voltages of 0.1−1.0 V, are easily obtained at moderate light intensity. However, the relationship between material structure and critical device properties, for example, short-circuit current density (J_{sc}), open-circuit voltage (V_{oc}), and carrier concentration, is still unclear in organic photocells. In organic materials, the intramolecular and intermolecular interactions are very different, with the latter being relatively weak van der Waals dispersion forces. The weak intermolecular forces allow for local structural disorder, and polymers may have amorphous and crystalline regions as well as chemical impurities.

Light absorption in bulk organics results in the formation of Frenkel excitons that are essentially localized on a single molecule with binding energies on the order of 0.1−1 eV. This leads to relatively low efficiency of charge separation.[3b] Therefore, in a homogeneous organic medium, only the higher energy absorptions are effective in charge generation. However, an efficient solar cell requires that charge generation be effective over the entire visible spectrum. Thus, tuning the absorption characteristics of the active material to the whole visible window is a desirable goal. Even though the mechanism of exciton dissociation has been under scientific investigation for decades,[1−8] enhancing the

* To whom correspondence should be addressed.
[†] Macromolecular Science & Engineering Center.
[‡] Department of Chemistry.

(1) (a) Chen, J. C.; Liu, C. J.; Ju, Y. H. *Sensors Actuators B* **2000**, *62*, 143−147. (b) McCullough, R. D.; Ewbank, P. C.; Loewe, R. S. *J. Am. Chem. Soc.* **1997**, *119*, 633−634. (c) Yu, G.; Srdanov, G.; Wang, J.; Wang, H.; Cao, Y.; Heeger, A. J. *Synth. Met.* **2000**, *111−112*, 133−137.

(2) (a) Bernius, M. T.; Inbasekaran, M.; O'Brien, J.; Wu, W. *Adv. Mater.* **2000**, *12*, 1737−1750. (b) Burrows, P. E.; Bulovic, V.; Forrest, S. R.; Sapochak, L. S.; McCarty, D. M.; Thompson, M. E. *Appl. Phys. Lett.* **1994**, *65*, 2922−2924. (c) Fou, A. C.; Onitsuka, O.; Ferreira, M.; Rubner, M. F.; Hsieh, B. R. *J. Appl. Phys.* **1996**, *79*, 7501−7509. (d) Gu, G.; Bulovic, V.; Burrows, P. E.; Forrest, S. R.; Thompson, M. E. *Appl. Phys. Lett.* **1996**, *68*, 2606−2608.

(3) (a) Assadi, A.; Svensson, C.; Willander, M.; Inganäs, O. *Appl. Phys. Lett.* **1988**, *53*, 195−197. (b)Forrest, S. R. *IEEE J. Sel. Top. Quantum Electron.* **2000**, *6*, 1072−1083. (c) Dimitrakapolous, C. D.; Malenfant, P. R. L. *Adv. Mater.* **2002**, *14*, 99−117.

(4) (a) Fukuda, M. *Optical semiconductor devices*; John Wiley & Sons: New York, 1998. (b) Roman, L. S.; Andersson, M. R.; Yohannes, T.; Inganäs, O. *Adv. Mater.* **1997**, *9*, 1164−1168. (c) Roman, L. S.; Mammo, W.; Pettersson, L. A. A.; Andersson, M. R.; Inganäs, O. *Adv. Mater.* **1998**, *10*, 774−777. (d) Yu, G.; Pakbaz, K.; Heeger, A. J. *Appl. Phys. Lett.* **1994**, *64*, 3422−3424. (e) Tan, L.; Curtis, M. D.; Francis, A. H. *Macromolecules* **2002**, *35*, 4628−4635.

(5) Binh, N. T.; Gailberger, M.; Bässler, H. *Synth. Met.* **1992**, *47*, 77−86.

(6) Halls, J. J. M.; Cornil, J.; dos Santos, D. A.; Silbey, R.; Hwang, D.-H.; Holmes, A. B.; Brédas, J. L.; Friend, R. H. *Phys. Rev. B* **1999**, *60*, 5721−5727.

(7) Silinsh, E. A.; Kolesnikov, V. A.; Muzikante, I. J.; Balode, D. R. *Phys. Status Solidi B* **1982**, *113*, 379−393.

(8) (a) Popovic, Z. D. *J. Chem. Phys.* **1982**, *76*, 2714−2719. (b)-Popovic, Z. D.; Hor, A.-M.; Loutfy, R. O. *Chem. Phys.* **1988**, *127*, 451−457.

10.1021/cm034183a CCC: $25.00
Published on Web 05/09/2003

charge separation efficiency of the neutral Frenkel exciton into free carriers is also a primary research goal. One method that may be used to enhance charge separation is to take advantage of the energy that can be generated when an electron is transferred from one substance to another, for example, at an interface. The interface may be a p/n junction, an electrode/active material surface, a different chemical substance, for example, C_{60}, homogeneously dispersed in a polymer matrix, or even an electroactive pendant group on the polymer main chain.[3b,5−7]

Previously, we have demonstrated that the photoconductive properties of a bilayer photodiode with two organic thin films, comprised of poly(3-butylthiophene) and a perylene diimide derivative sandwiched between two electrodes, were highly affected by charge-transfer reagents attached to the side chain of the polymer.[4e] P3AT is a p-type organic material and can be processed easily to form free-standing films that may be doped by various methods, thereby providing easy control of carrier concentration in the bulk material. Moreover, the energy levels (HOMO and LUMO) of P3AT can be changed by varying the side chain stereo-regularity (control of side chain morphology),[11,12] by changing the electron-donating properties of the side chains, and by copolymerizing other components into the main chain, or any combination of these strategies.

This paper discusses characteristics of bilayer photocells fabricated from derivatives of P3AT, for example, regiorandom poly(3-butylthiophene), regioregular poly(3-octylthiophene), and poly(3-butylthiophene-*co*-EDOT). In the latter material, 3,4-ethylenedioxythiophene, EDOT, which is very easily oxidized (low ionization energy), was copolymerized with 3-butylthiophene. For the p/n junctions, 1,2-diaminobenzene perylene-3,4,9,-10-tetracarboxylic acid diimide (PV) was used as the

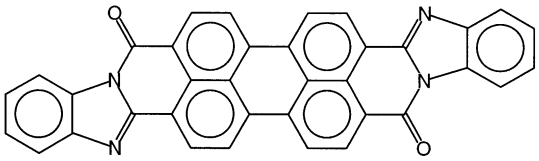

PV

n-type material,[13,14] and the poly(thiophene)s were used as the p-type materials.

Experimental Section

Syntheses were performed under a nitrogen atmosphere using standard Schlenk line techniques. Reagents were purchased and used as received unless otherwise stated. Regioregular P3OT was synthesized according to the literature methods.[11] Uniform films were deposited on the indium tin oxide-coated glass (ITO, 15 Ω/square) by spin-coating polymer solutions in chloroform (12−15 mg/mL). Film thickness (between 120 and 150 nm) was measured by a Dektak-3 surface profilometer. PV was deposited to a thickness of 50−100 nm by vacuum evaporation. The deposition rate was 25 Å/s at a pressure of 10^{-6}−10^{-5} Torr. The average device area was 0.25 cm^2. Electrical measurements were carried out under illumination by a Xenon lamp, the intensity of which was monitored with a power meter. A GCA/McPherson monochromator was used to provide monochromatic light to record the diode response under a specific excitation wavelength. The data were scanned by a Keithley 617 electrometer and recorded through a PCI-GPIB card (National Instruments Corporation) into the computer.

Synthesis of 2,5-Dibromo-3,4-ethylenedioxythiophene. A 100-mL Schlenk flask equipped with a stir bar and N_2 inlet/outlet was charged with 3,4-ethylenedioxythiophene (EDOT) (14.08 mmol, 2.0 g), NBS (30.96 mmol, 5.3 g), and chloroform/acetic acid mixture (20 mL/30 mL). The reaction was allowed to run at room temperature for 2 h. The mixture was washed with hot water. The organic layer was extracted by CH_2Cl_2. Dark blue solid (3.4 g, 81.0% yield) was recovered after removing the organic solvent with a Rotavap. ^{1}H NMR ($CDCl_3$): δ 4.20 (4H, s).

Synthesis of Poly(3-butylthiophene-*co*-ethylenedioxythiophene) (P3BT-*co*-EDOT). A 100-mL Schlenk flask equipped with a condenser, stir bar, and N_2 inlet/outlet was charged with 2,5-dibromo-3,4-ethylenedioxythiophene (0.667 mmol, 0.20 g), 2,5-dibromo-3-butylthiophene (2.68 mmol, 0.80 g), $Ni(COD)_2$ (4.18 mmol, 1.15 g), and 2, 2′-bipyridyl (4.60 mmol, 0.74 g) in anhydrous THF (50 mL). The mixture was heated to reflux temperature overnight, and the mixture was then poured into 300 mL of MeOH to which several milliliters of concentrated HCl had been added. The solid that precipitated was collected by filtration and then dissolved in $CHCl_3$. After filtration through a 5-mm layer of Celite, the filtrate was concentrated on a rotary evaporator, and the product was reprecipitated by pouring the $CHCL_3$ solution into acidified MeOH. The precipitate was collected and extracted sequentially with hexane and acetone in a Soxhlet apparatus. These extracts were discarded. The solid was then extracted into $CHCl_3$. The product was precipitated by pouring the $CHCl_3$ solution into MeOH (300 mL). A black-red solid (0.288 g, 61.7% yield) was recovered by filtration. ^{1}H NMR ($CDCl_3$): δ 6.8−7.2 (1H, s-ring proton), 4.2−4.5 (1H, EDOT bridge protons), 2.4−2.9 (2H, α-methylene protons), 1.2−1.9 (4H, β- and γ-methylene protons), 0.6−0.9 (3H, methyl protons). λ_{max}(abs) = 440 nm (CH_2Cl_2); 470 nm (Film). λ_{max}(em) = 570 nm (CH_2Cl_2). λ_{max}(ex) = 440 nm (CH_2Cl_2). M_n, 64400; M_w, 170000; PDI = 2.64. Anal. Calcd for P3BT-*co*-EDOT: C, 64.98; H, 6.14. Found: C, 64.67; H, 6.46. TGA analysis (N_2): 5% weight loss at 417 °C; 40% weight loss at 599 °C.

Results and Discussions

Material Synthesis. In the synthesis of regiorandom P3BT and P3BT-*co*-EDOT, the monomers, 2,5-dibromo-3-butylthiophene and 2,5-dibromo-3,4-ethylenedioxythiophene (2,5-dibromo-EDOT), were coupled by reactions with a Ni^0 complex, $Ni(COD)_2$. The ratio of head-to-tail versus head-to-head coupling is determined by the Ni(0) coupling reaction and is typically about 70% HT.[15] The copolymerization is illustrated in Scheme 1. The composition of EDOT in the final copolymer was nearly the same as the ratio in the initial feed. It has been our experience with Ni(0) coupling reactions that random copolymers result from this copolymerization method.

Energy Diagrams of Photodiodes. The incorporation of EDOT into the poly(3-butylthiophene)s affected

(9) Arkhipov, V. I.; Emelianova, E. V.; Bässler, H. *Phys. Rev. Lett.* **1999**, *82*, 1321−1324.
(10) Rothberg, L. J.; Yan, M.; Fung, A. W. P.; Jedju, T. M.; Kwock, E. W.; Galvin, M. E. *Synth. Met.* **1997**, *84*, 537−538.
(11) McCullough, R. D.; Lowe, R. D. *J. Chem. Soc., Chem. Commun.* **1992**, 70−72.
(12) Chen, T.-A.; Wu, X.; Rieke, R. D. *J. Am. Chem. Soc.* **1995**, *117*, 233−244.
(13) Maki, T.; Hashimoto, H. *Bull. Chem. Soc. Jpn.* **1952**, *25*, 411−413.
(14) Hiramoto, M.; Fukusumi, H.; Yokoyama, M. *Appl. Phys. Lett.* **1992**, *61*, 2580−2582.
(15) Politis, J. K.; Nemes, J. C.; Curtis, M. D. *J. Am. Chem. Soc.* **2001**, *123*, 2537−2547.

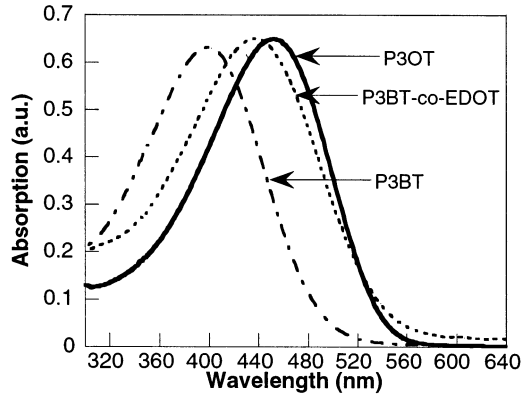

Figure 1. UV−vis spectra of polymers in chloroform.

Scheme 1. Synthesis of P3BT-*co*-EDOT via Ni(0) Coupling Reaction

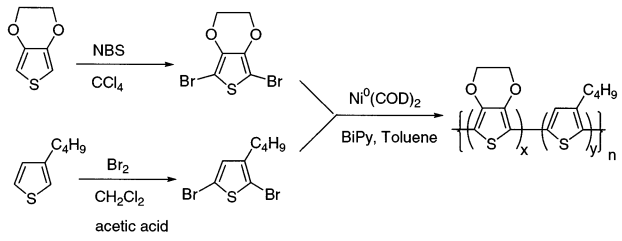

the spectral properties of the polymer. Figure 1 shows the UV−vis spectra of solutions of P3BT (regiorandom), P3BT-*co*-EDOT, and P3OT (regioregular). The peak at 400−420 nm shifts to longer wavelength (a) upon the incorporation of EDOT group, (b) on going from solution to solid state, and (c) as the regioregularity increases. The two latter trends are characteristic of the $\pi-\pi^*$ transition of P3ATs.

In a cyclic voltammogram, P3BT showed an oxidation potential of 0.4 V vs ferrocene/ferrocenium couple, which corresponds to an ionization energy of 5.2 eV referenced to the vacuum.[16] The optical band gap, E_g, was determined to be 2.5 eV by extrapolating the optical absorption edge to the baseline ($\lambda_{edge} = 500$ nm). The LUMO energy is thus estimated to be at −2.7 eV vs the vacuum level. According to these energy level data and data for PV from the literature,[14] ITO and Ag were chosen as the electrodes for the p/n junction devices. Ohmic contacts will form on the p-side for holes, Figure 2a, and on the n-side for electrons. However, these contacts become Schottky type for opposite carriers, that is, electron injection on the p-side or hole injection on the n-side.

By incorporation of a strong electron-donating element (EDOT) into the polythiophene main chain, the P3BT-*co*-EDOT copolymer has a further decreased oxidation potential (0.0 V vs ferrocene/ferrocenium couple or 4.8 eV vs vacuum), as well as a decreased energy barrier between the polymer and ITO ($\phi_0 = 4.8-4.8 = 0.0$ eV). The E_g was reduced to 1.91 eV ($\lambda_{edge} =$ 650 nm), giving a LUMO energy 2.9 eV below the vacuum level.

Regioregular, P3OT, shows oxidation at a similar potential as regiorandom P3BT, placing the HOMO energy at 5.2 eV; however, because of the increased

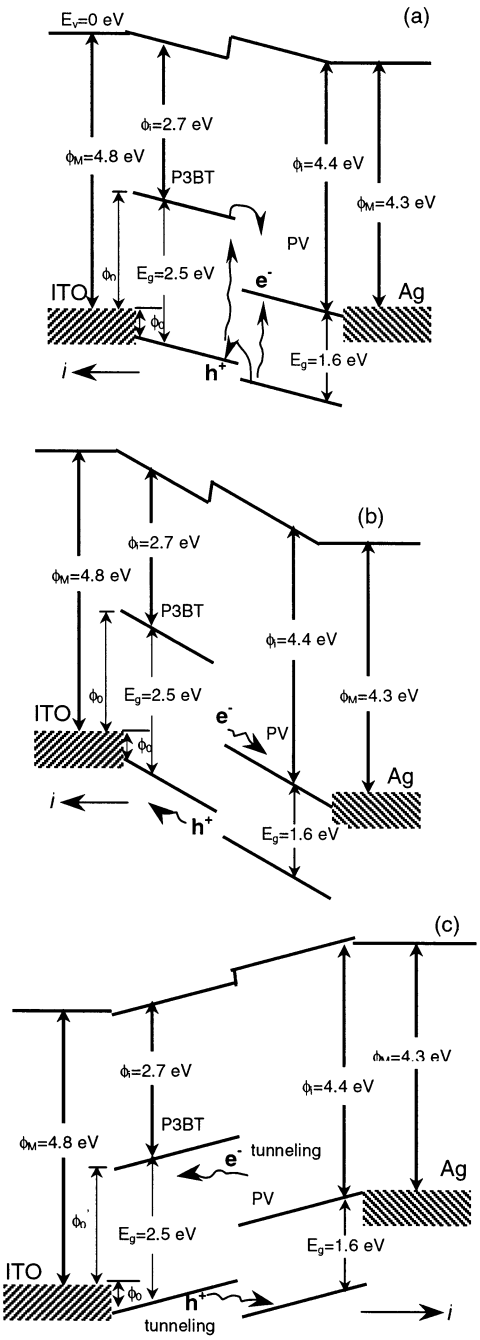

Figure 2. Energy structure of a ITO/P3BT/PV/Ag device; photocurrent direction was indicated on the corner: (a) short-circuit situation, wavy arrows represent the process of charge generation described in the text; (b) reverse bias; (c) forward bias, where electron and hole tunneling is represented by wavy arrows.

effective conjugation length in the regioregular polymer, the optical absorption starts at 650 nm, giving an optical band gap of 1.91 eV, thus placing the LUMO level at 3.3 eV below the vacuum.

Photoconduction Properties. Three diode structures were studied consisting of p/n bilayers, ITO/P3BT/PV/Ag, ITO/P3BT-*co*-EDOT/PV/Ag, and ITO/P3OT/PV/Ag. $J-V$ curves (dark and photoexcited through the ITO side) of the first two devices are shown in Figure 3, where characteristics of photodiode behavior were observed. The devices based on P3BT-*co*-EDOT and P3OT had a greater short-circuit current, I_{sc}, than that for

(16) Wu, C.-C.; Sturm, J. C.; Register, R. A.; Tian, J.; Pana, E. P.; Thompson, M. E. *IEEE Trans. Electron Devices* **1997**, *44*, 1269−1281.

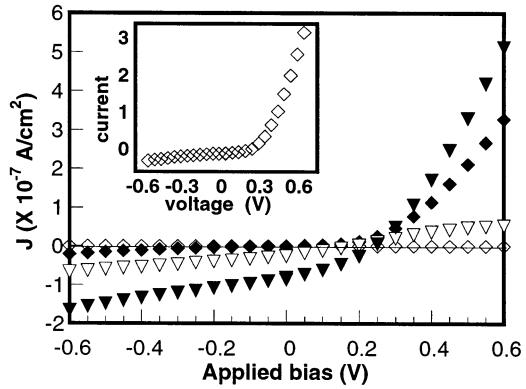

Figure 3. $J-V$ curves of devices in the dark (diamonds) and under 468 nm illumination (triangles). ITO/P3BT-*co*-EDOT/PV/Ag (filled); ITO/P3BT/PV/Ag (open). The inset is an expanded *y*-axis plot of the dark current for the P3BT device.

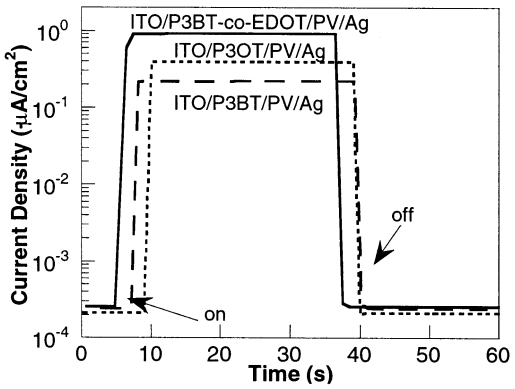

Figure 4. Steady-state short-circuit current of photodiodes with white light illumination (3.8 mW/cm^2).

P3BT/PV devices (Figure 4), probably due to the better conductivity of the latter two polymers. The measured monochromatic power conversion efficiency at 468 nm (10 μW/cm^2) for an ITO/P3BT-*co*-EDOT/PV/Ag bilayer device was 0.1% (V_{oc} = 0.25 V, J_{sc} = 0.12 μA/cm^2, FF (fill factor) = 0.34).

Action spectra, shown in Figure 5, of the short-circuit photocurrent responses covered the entire visible window (400−800 nm) for all polymeric bilayer devices. The action spectra for P3BT and P3BT-*co*-EDOT devices in the longer wavelength region resemble the absorption spectrum of the PV. However, when illuminated from the ITO side, wavelengths near 500 nm, where the absorption spectra of P3BT and PV overlap, appear to be more effective in producing charge carriers in relation to the shape of the *PV* absorption spectrum and wavelengths near the λ_{max} for P3BT are not so effective. Since the light arriving at the p/n junction traverses the polymer layer, we postulate that most of the light in the region, 400−500 nm, that is, near the λ_{max} of P3BT, is absorbed by the polymer before it reaches the p/n junction. Thus, there is little light in this spectral region available to generate carriers at the p/n interface.

This hypothesis is supported by the action spectra of ITO/P3BT-*co*-EDOT/PV/Au device, where a strong photoresponse in the polymer absorption region was observed when the device was illuminated through the semitransparent Au electrode, but when illuminated through the ITO side, the action spectrum again resembled the PV absorption spectrum. Therefore, the

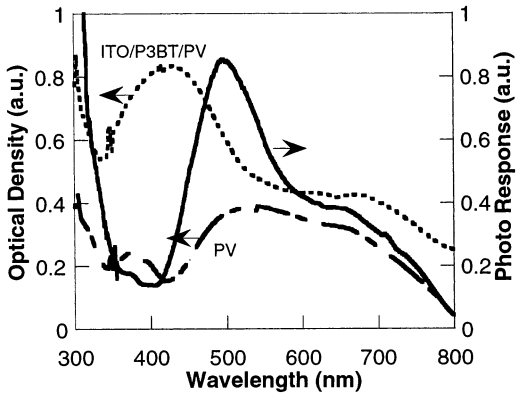

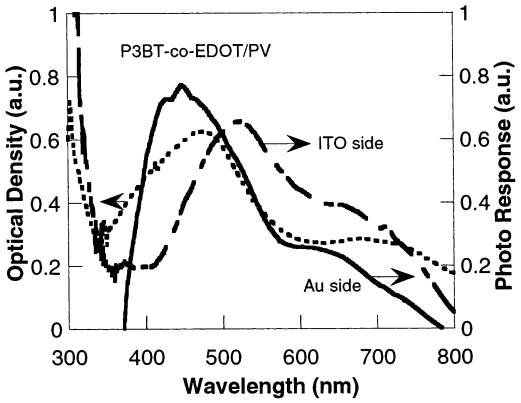

Figure 5. Action spectra of ITO/P3BT/PV/Ag (top) and ITO/P3BT-*co*-EDOT/PV/Au (bottom). (Top) Dotted and dashed lines represent optical absorption of ITO/P3BT/PV and PV, respectively; (bottom) dotted line represents optical absorption of ITO/P3BT-*co*-EDOT/PV and solid and dashed lines represent photo response with illumination from Au or ITO, respectively.

action spectra demonstrate that the p/n junction is a locus of carrier photogeneration. Furthermore, polymers can be combined with PV to function as solar cells that absorb wavelengths over the visible range.

As shown in Figure 2, carrier generation at the p/n junction can occur in either of two ways. An exciton formed by absorption of a photon by the polymer within some distance, L, of the interface can dissociate efficiently and exothermically by transferring an electron to the LUMO of a PV molecule near the interface. This charge separation process places an electron in the n-type PV and a hole in the p-type polymer. Similarly, if a PV molecule within the distance L' of the polymer/PV interface absorbs a photon, the resulting exciton can exothermically transfer a hole to the LUMO of a polymer molecule near the interface. The latter process also results in charge separation, with the positive carrier in the polymer and the negative carrier in the PV. Excitons generated outside the interface layer, $L-L'$, can diffuse into this boundary layer and dissociate into carriers, but the probability of their doing so drops off rapidly with the distance that must be traversed to reach the boundary layer. Under the built-in bias or under reverse bias, the electron is swept toward the metal (back) electrode, and the hole is swept toward the ITO as shown in Figure 2a,b.

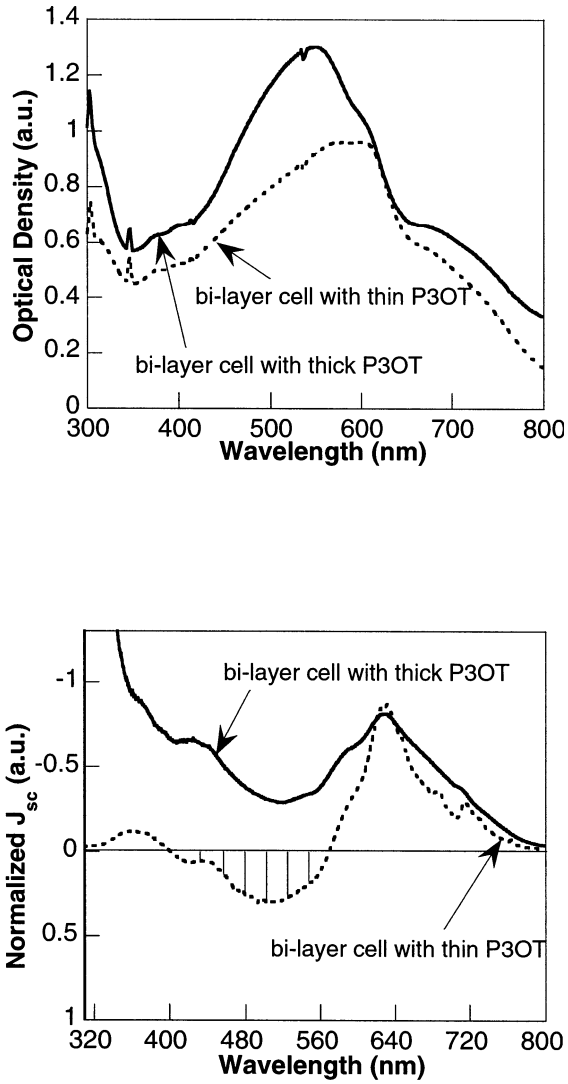

Figure 6. (top) Absorption spectra of ITO/P3OT/PV/Ag photocell with polymer layers of different thicknesses; (bottom) action spectra (J_{sc}) of these bilayer devices under illumination crossing the whole visible wavelength. Shaded area represents the wavelength range in which the sign of I_{sc} changes.

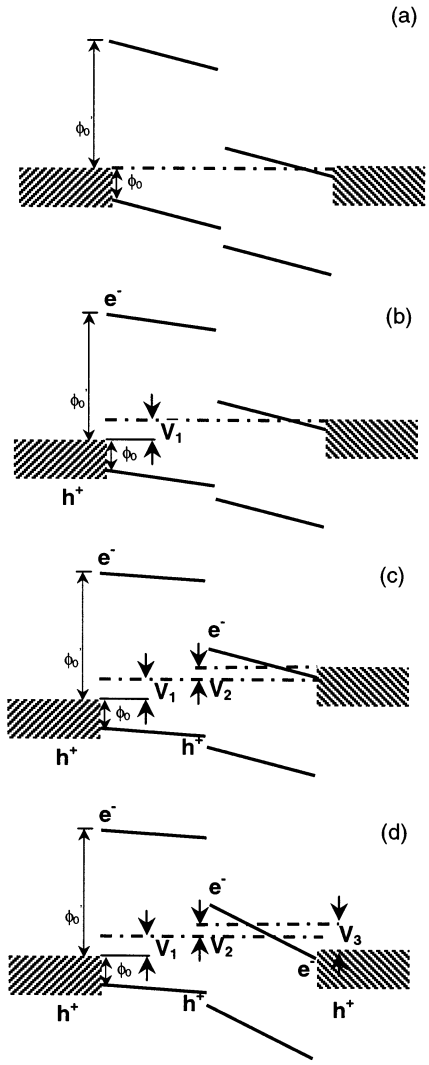

Figure 7. Energy diagram of a ITO/P3BT/PV/Ag device at open circuit: (a) dark equilibrium ($V_{oc} = 0$); (b) photoinjection from the ITO/P3BT interface only ($V_{oc} = V_1$); (c) photogeneration at both ITO/P3BT and P3BT/PV interfaces ($V_{oc} = V_1 + V_2$); (d) photogeneration at all the interfaces ($V_{oc} = V_1 + V_2 - V_3$).

However, the energy scheme shown in Figure 2 cannot be used to explain the magnitude or behavior of the open-circuit voltage (V_{oc}), as exemplified by the change in sign of the short-circuit current density (J_{sc}) that was observed for some devices constructed with thin polymer layers (Figure 6). Figure 7 represents an adaptation of the model developed by Bonham for explaining the magnitude and sign of the open-circuit voltage during steady-state illumination of an organic photodiode.[17] In drawing the energy levels shown in Figure 7, it is assumed that the organic materials are insulators with no dopants deliberately added so that dark current due to intrinsic carriers can be ignored and that the rate of carrier photogeneration in the bulk material is negligible compared to the rate of generation at interfaces.

In an insulator, the quasi-Fermi level (E_{fp} or E_{fn}) is flat throughout the insulator, that is, $dE_{fp}/dx = 0$ in the polymer layer and $dE_{fn}/dx = 0$ in the PV layer at open-circuit.[17] Figure 7a represents an energy diagram of the bilayer device in the dark after equilibration of the Fermi levels and where the relative positions of energy levels of all the materials are the same as those shown in Figure 2. Equilibrium is established by transfer of electrons across the insulators, such that the quasi-Fermi levels in both layers are then equal to the Fermi levels of the two electrodes, Figure 7a.

According to Bonham, charge separation occurs at the interfaces and is maintained by continuous illumination. Suppose only the ITO/polymer interface is illuminated (no illumination reaches polymer/PV and PV/Ag interfaces) and dissociation of the exciton at the electrode leads to net electron injection from the ITO to the polymer surface. Then, E_{fp} must rise relative to E_i at the polymer surface, where E_i is the intrinsic Fermi level and lies in the middle of the gap and E_{fp} is the quasi-Fermi level in the p-type polymer. E_{fp} and E_{fn} remain fixed relative to each other and are equal to the Fermi level of the Ag electrode since the other two interfaces have not been illuminated. There is then a difference in Fermi levels between the two electrodes, equal to the discontinuity at the illuminated surface. This difference

(17) Bonham, J. S. *Aust. J. Chem.* **1976**, *29*, 2123−2136.

is the observed photovoltage ($V_{oc} = V_1$, Figure 7b). If light penetrates from the ITO to the organic/organic interface, the excitons in the boundary layers dissociate as described above and electrons are injected into the PV and holes into the polymer. E_{fn} rises relative to E_{fp} at the interface and $E_{fn}^{(PV)} - E_{fp}^{(PT)} = qV_2$. The Fermi level of the Ag electrode remains fixed relative to E_{fn}, and $V_{oc} = V_1 + V_2$, Figure 7c.

Finally, if the PV/Ag interface receives illumination, then photoinjection of electrons from Ag to the PV will cause the Fermi level of the Ag electrode to descend and the overall photovoltage is then $V_{oc} = V_1 + V_2 - V_3$ as shown in Figure 7d. Obviously, the photoelectron injection at the back electrode will change the sign of the open-circuit voltage if $V_3 > V_1 + V_2$. Voltage reversal may occur under the following conditions: (a) a significant amount of light penetrates to the PV/Ag interface, (b) effective photoinjection of electron from Ag to the LUMO of the PV occurs, and (c) the wavelength of excitation does not lead to extensive photogeneration at ITO/polymer and polymer/PV interfaces. Physically, the sign change of the photovoltage also signals a sign change in short-circuit current.

Figure 6 shows such a reversal of sign of the J_{sc} for the ITO/P3OT/PV/Ag device with illumination from the ITO side when a thin polymer film was used. The short-circuit current spectrum of the thick polymer layer device is similar to the action spectra of P3BT and P3BT-*co*-EDOT bi-layer devices, where the organic/organic interface is an efficient region for carrier generation. Electrons flow from the p/n junction through the PV to the Ag electrode, and holes flow from the interface through the polymer to the ITO. Externally, the current direction (flow of holes) is from the ITO to the Ag. In the diode with the thin polymer layer, the sign of J_{sc} is opposite to that of the thick layer device when illuminated with light in the region $\lambda = 400-600$ nm. These wavelengths correspond to the region of strong absorption by the polymer so that very little light with these wavelengths reaches the back electrode if the polymer film is thick. With a thin P3OT layer, most of the light of this wavelength passes through the polymer, and the absorption coefficient of the PV is low in this wavelength region. Hence, this light penetrates to the Ag electrode, leading to significant electron injection and an increase of V_3, leading to sign reversal of V_{oc} and J_{sc}.

The efficiency of photoinjection of carriers from the electrodes to the organic insulators is related to the energy level differences between them. Thus, V_{oc} is dependent not only on the selection of electrodes and organic materials but also on the thickness of the layers and the illumination wavelength and intensity. This situation is quite different from that which obtains with classic photodiodes based on doped inorganic semiconductors, where V_{oc} is determined by the difference in the Fermi levels of the p- and n-doped materials, $qV_{oc} = E_{fi} - E_{fp}$.[18]

Figure 8 shows the net photo response of ITO/P3BT-*co*-EDOT/PV/Au at different biases with illumination from the ITO or Au side. These wavelengths correspond to the maximum absorption of the polymer (450 nm),

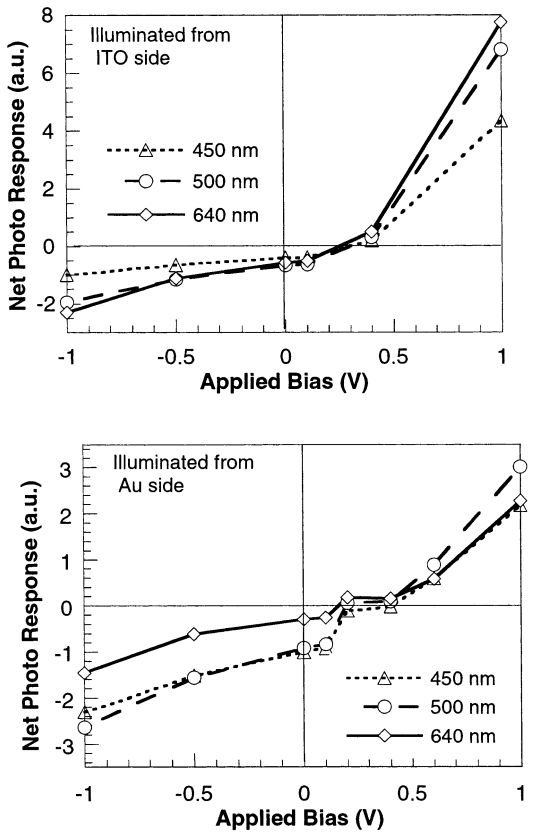

Figure 8. Electric field dependence of photoconduction in ITO/P3BT-*co*-EDOT/PV/Au at different illumination wavelengths.

interface (500 nm), and PV (640 nm); the response has been corrected for the different light intensities of the Xe lamp at the different wavelengths. Generally, the photo response increases with increasing electric field under both forward and reverse bias, regardless of the illumination wavelength or direction. If carriers were generated primarily at the p/n junction, then one would expect that the highest photocurrent would result from illumination with wavelengths that are most strongly absorbed in the p/n layer ($\lambda = 500$ nm). However, as Figure 8 shows, light with $\lambda = 640$ nm is slightly more effective than the $\lambda = 500$ nm light when the device is illuminated through the ITO electrode. We ascribe this effect to the fact that the 640 nm light is absorbed by the PV adjacent to the charge dissociation zone (the p/n junction). The excitons generated near the interface can diffuse to the p/n junction where they dissociate into free carriers. Conversely, the 450 nm light is most strongly absorbed near the ITO electrode, and these excitons will decay before diffusing all the way across the polymer layer. When the illumination is through the Au electrode, the 640-nm light is most strongly absorbed near the Au electrode, and now the excitons formed at the PV/Au layer must diffuse to the interface. The 500-nm light is now strongly absorbed at the p/n junction, leading to efficient carrier generation.

Figure 9 shows that the photocurrents obey a power law dependence of the light intensity, $J \sim I^k$. The concentration of carriers is related to the current density through eq 1, where n is the carrier concentration (cm^{-3}), τ is the carrier lifetime, R is the the rate constant for the bimolecular recombination of photogenerated holes and electrons, and g is the the carrier generation

(18) Sze, S. M. *Physics of Semiconductor Devices*, 2nd ed.; John Wiley & Sons: New York, 1981.

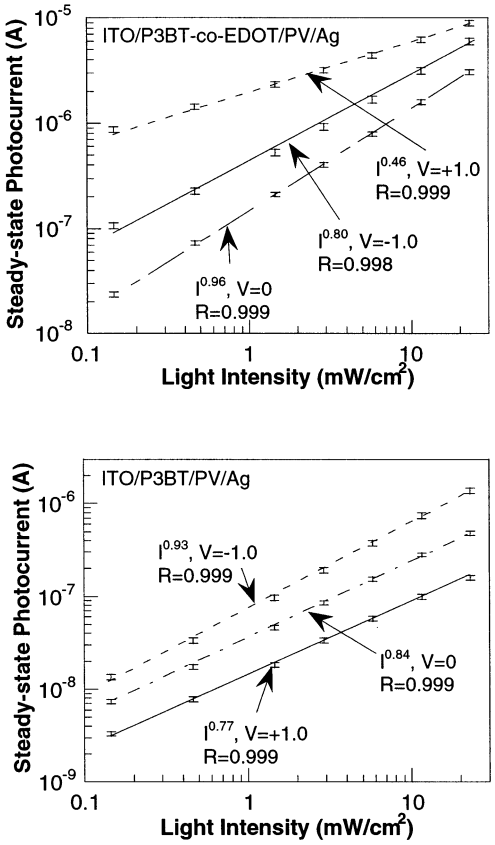

Figure 9. Light intensity dependence of photocurrent: (top) ITO/P3BT-*co*-EDOT/PV/Ag; (bottom) ITO/P3BT/PV/Ag.

rate, given in eq 2, where φ is the carrier quantum yield, I_0 is the incident photon flux, d is the thickness of the organic layers, and l is the width of the of the interfacial boundary layer in which exciton dissociation occurs. Since the concentration of holes generated at the interface equals the concentration of electrons, the bimolecular term is proportional to the square of the carrier concentration.

$$\frac{\mathrm{d}n}{\mathrm{d}t} = g_n - \frac{n}{\tau_n} + \frac{1}{q}\frac{\mathrm{d}j_n}{\mathrm{d}x} - Rn^2 = 0 \qquad (1)$$

$$g = \frac{\phi(I_\mathrm{d} - I_\mathrm{l})A}{Al} = \frac{\phi[I_0\mathrm{e}^{-\alpha d} - I_0\mathrm{e}^{-\alpha(d+l)}]}{l} = \frac{\phi I_0\mathrm{e}^{-\alpha d}(1 - \mathrm{e}^{-\alpha l})}{l} \qquad (2)$$

If the rate of carrier extraction via the external circuit is small compared to the first- and second-order decay rates, then at steady state

$$\mathrm{d}n/\mathrm{d}t = 0 = g - n/\tau - Rn^2 \qquad (3)$$

If the bimolecular term is small compared to $(g - n/\tau)$, then $n_{ss} = g\tau = AI_0^1$, and the steady-state current ($J_{ss} \approx n_{ss}d$) is also proportional to the first power of the incident photon flux. This situation is obtained when the external bias is less than or equal to zero. In these instances, the internal field sweeps the electrons away from the polymer/PV interface toward the Ag ("back") electrode while sweeping the holes toward the ITO. The electrons and holes are rapidly separated and do not recombine at an appreciable rate (cf. Figure 2a,b).

On the other hand, under positive bias, the photogenerated electrons and holes must tunnel through their respective barriers at the polymer/PV interface (see Figure 2c). The high concentration of holes and electrons at the interface promotes bimolecular recombination, and $Rn^2 \gg n/\tau$ so that $n_{ss} = (g/R)^{1/2}$ and $J_{ss} \sim I_0^{1/2}$, as observed.

Chemical Doping of the Polymer Layer. One advantage of using poly(thiophene)s is the relative ease of changing the carrier concentration by doping the polymer with chemical reagents, such as iodine. Even though there are many research reports on iodine doping to achieve high conductivity in conjugated polymers,[11,19−21] the stability of I_2-doped materials is not high, especially if the doped material is open to the atmosphere or is placed under vacuum. Under these conditions, the volatile I_2 sublimes from the polymer and the dopant level decreases or disappears altogether. Therefore, iodine doping is not an appropriate way to improve performance in photocells that require a high vacuum (10^{-6}−10^{-5} Torr) during their fabrication.

We therefore investigated the photoconduction characteristics of devices in which the polymer layer was treated with vacuum-stable dopants, such as strong acids or nitrosonium tetrafluoroborate. The P3OT film, precast onto ITO, was immersed into acid (pH = 3, aqueous solution of HCl, H_2SO_4, or toluenesulfonic acid) or into a solution of $NOBF_4$ in anhydrous acetonitrile for 30 s, followed by rinsing with distilled water (for acid-doped samples) or vacuum-drying (for $NOBF_4$-doped films).

Figure 10 shows the influence of these dopants on the UV−vis absorption spectrum of the P3OT film. The intensity of the π−π^* transition peak at 520 nm[11,12] decreases and shifts slightly to the blue as neutral polymer is converted to the oxidized form. Except in the HCl-doped samples, new, broad peaks around 700−900 nm appeared in the acid-doped films, and it appears that an additional peak (>1100 nm) is present in $NOBF_4$-doped samples. These new peaks are due to transitions to and from the singly occupied highest molecular orbital (SOMO) of the oxidized polymer.[15,22−25]

The acid-doped films proved to be unsuitable for device fabrication because the strong affinity of aqueous acid solutions for the ITO substrate caused the acid-doped P3OT films to lose mechanical and electrical contact with the ITO electrode. No such problems were found with the $NOBF_4$-doped samples, and the doping level was easily controlled by adjusting the dopant

(19) Naka, K.; Uemura, T.; Chujo, Y. *Macromolecules* **2000**, *33*, 6965−6969.
(20) Tashiro, K.; Kobayashi, M.; Kawai, T.; Yoshino, K. *Polymer* **1997**, *38*, 2867−2879.
(21) Parakka, J. P.; Chacko, A. P.; Nikles, D. E.; Wang, P.; Hasegawa, S.; Maruyama, Y.; Metzger, R. M.; Cava, M. P. *Macromolecules* **1996**, *29*, 1928−1933.
(22) McCullough, R. D.; Lowe, R. D.; Jayaraman, M.; Anderson, D. L. *J. Org. Chem.* **1993**, *58*, 904−912.
(23) Abdou, M. S. A.; Lu, X.; Xie, Z. W.; Orfino, F.; Deen, M. J.; Holdcroft, S. *Chem. Mater.* **1995**, *7*, 631−641.
(24) Zagorska, M.; Kulszewicz-Bajer, I.; Pron, A.; Sukiennik, J.; Raimond, P.; Kajzar, F.; Attias, A.-J.; Lapkowski, M. *Macromolecules* **1998**, *31*, 9146−9153.
(25) Brédas, J. L.; Beljonne, D.; Cornil, J.; Calbert, J. P.; Shuai, Z.; Silbey, R. *Synth. Met.* **2001**, *125*, 107−116.

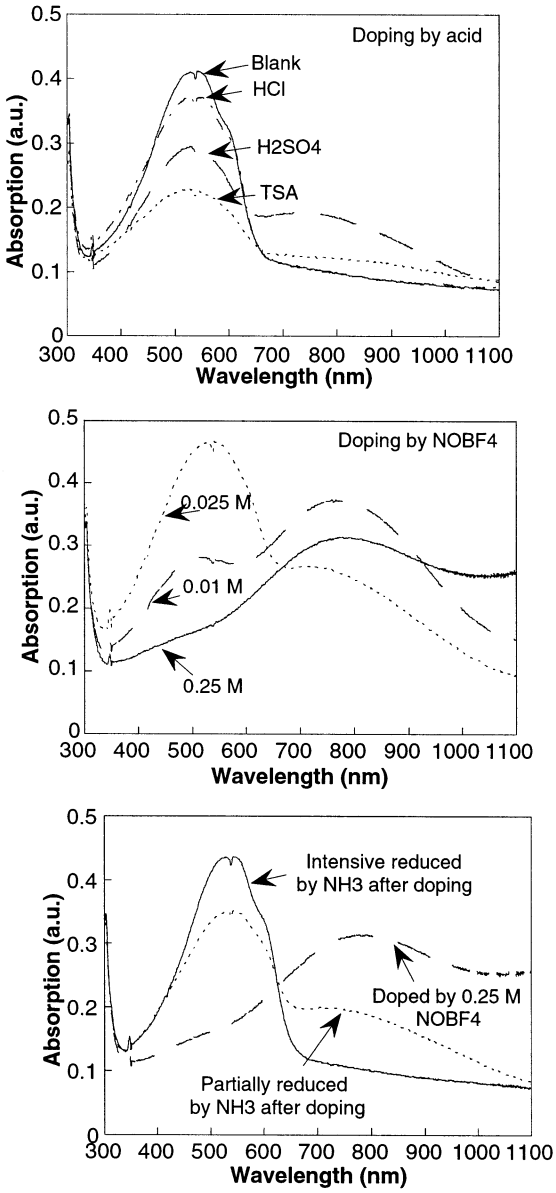

Figure 10. UV−vis spectra of (top) P3OT films doped with aqueous acids, (middle) $NOBF_4$ at different concentrations, and (bottom) $NOBF_4$-doped P3OT films treated with NH_3 gas.

concentration. Clearly, the new peak at 700−900 nm becomes stronger with more concentrated dopant (Figure 10, middle), and the deeply doped polymer can be partially or fully reduced by NH_3 vapor (Figure 10, bottom) according to the NH_3 exposure time. This reversibility demonstrates that the $NOBF_4$ doping only involves reversible electron transfer without structure-altering, irreversible chemical reactions (e.g., nitration).

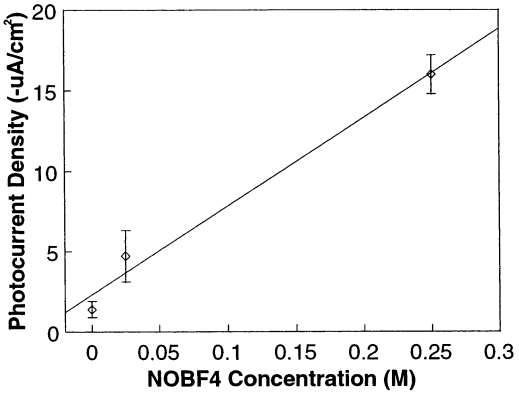

Figure 11. Effect of $NOBF_4$ dopant concentration on the short-circuit current density with xenon arc lamp illumination.

PV was vacuum-deposited onto the $NOBF_4$-doped (0.025 and 0.25 M $NOBF_4$) P3OT layers to form bilayer p/n junction devices. The short-circuit current density (J_{sc}) increased by nearly 1 order of magnitude with doping (Figure 11); however, only minor changes (0.2−0.35 V) were observed in the open-circuit voltage. No significant changes in these measurements were observed after storing these devices on the shelf in the ambient environment for a month.

Conclusions

Bilayer photocells based on P3AT-type polymers and copolymers as the p-type layer and a perylene diimide (PV) as the n-type layer were characterized. Current−voltage characteristics, as a function of incident light wavelength and intensity, and cell dimensions show that the polymer/PV interface, as well as the electrode/organic interfaces, are the major loci of carrier photogeneration. A study of the dependence of photocurrent on light intensity showed that, depending on the materials and applied bias, either unimolecular (lifetime determined, $J \sim I^{1.0}$) or bimolecular (recombination dominant, $J \sim I^{0.5}$) routes to charge carrier decay are obtained. Doping of regioregular P3OT by various aqueous acids and $NOBF_4$ showed that carrier concentration in the polymer can be controlled, and higher photocurrents were obtained in doped samples. More interestingly, $NOBF_4$-doped polymer films are very stable under vacuum and ambient conditions. Thus, $NOBF_4$ doping is an attractive route for improving the efficiency of organic photocells.

Acknowledgment. The authors gratefully acknowledge the financial support from NSF (Grant No. DMR-9986123). Programming assistance by Dr. Steve Parus is gratefully acknowledged.

CM034183A